

# BMSCs and Pectin-Based E2-Loaded Microcapsules with Injectable Pectin-Pluronic<sup>®</sup> F-127 Scaffolds for Mouse Endometrial Regeneration Application

**Yuelin Wu**

Tongji University School of Medicine

**Shengyi Gu**

Tongji University School of Medicine

**Jonathan M. Cobb**

Milwaukee School of Engineering

**Griffin H. Dunn**

Milwaukee School of Engineering

**Taylor A. Muth**

Milwaukee School of Engineering

**Chloe J. Simchick**

Milwaukee School of Engineering

**Baoguo Li**

University of Shanghai for Science and Technology

**Wujie Zhang**

Milwaukee School of Engineering

**Xiaolin Hua** (✉ [xiaolin\\_hua@tongji.edu.cn](mailto:xiaolin_hua@tongji.edu.cn))

Tongji University School of Medicine <https://orcid.org/0000-0003-1098-5010>

---

## Research Article

**Keywords:** Endometrial regeneration, Bone marrow-derived mesenchymal stem cells, Pectin-based E2-loaded Microcapsules, Pectin-Pluronic<sup>®</sup> F-127 scaffolds, Exosomes

**Posted Date:** December 9th, 2021

**DOI:** <https://doi.org/10.21203/rs.3.rs-1091969/v1>

**License:**   This work is licensed under a Creative Commons Attribution 4.0 International License.

[Read Full License](#)

---

# Abstract

## Background

Uterine endometrium is a highly dynamic tissue which consists of a basal layer and a functional layer. Bone marrow-derived mesenchymal stem cells (BMSCs) have been recognized as new candidates for the treatment of serious endometrial injuries. However, due to the local microenvironment of damaged endometrium, transplantation of BMSCs yielded disappointing results with respect to survival, attachment, differentiation, and proliferation.

## Methods

Pectin-Pluronic® F-127 scaffolds were fabricated. E2 was encapsulated into the W/O/W microspheres to construct pectin-based E2-loaded microcapsules (E2 MPs). The BMSCs/E2 MPs/scaffolds system was then injected into the uterine cavity of mouse endometrial injury model. Furthermore, the mechanism of E2 in promoting the repair of endometrial injury was also investigated.

## Result

Pectin-Pluronic® F-127 scaffolds could provide three-dimensional architecture for the attachment, growth, and migration of BMSCs. E2 MPs has the potential to serve as a long-term reliable source of E2 for endometrial regeneration. At four weeks after transplantation, it was demonstrated that the system increased proliferative abilities of uterine endometrial cells, facilitated microvasculature regeneration, and restored the ability of endometrium to receive an embryo, suggesting that the BMSCs/E2 MPs/scaffolds system is a promising treatment option for endometrial regeneration. Exosomes are critical paracrine mediators that act as biochemical cues to direct stem cell differentiation. In this study, it was found that the expression of endometrial epithelial cells (EECs) markers was up-regulated in BMSCs treated by exosomes secreted from endometrial stromal cells (ESCs-Exos). Exosomes derived from E2-stimulated ESCs further promoted the expression level of EECs markers in BMSCs, suggesting exosomes released from ESCs by E2 stimulation could enhance the differentiation efficiency of BMSCs.

## Conclusion

The BMSCs/E2 MPs/scaffolds therapeutic strategy may be beneficial in the treatment of severely damaged endometrium. Exosomes derived from ESCs play paracrine roles in endometrial regeneration stimulated by E2, potentially modulating the differentiation of BMSCs.

## 1. Introduction

Uterine endometrium is a highly dynamic tissue which consists of a basal layer and a functional layer<sup>[1,2]</sup>. Severe damage to the basal layer caused by curettage, infections, caesarean section and myomectomy lead to endometrium scar formation or intrauterine adhesion (IUA), which may result in amenorrhea, hypomenorrhea, recurrent pregnancy loss, or infertility<sup>[3,4]</sup>. Several strategies, such as hysteroscopic surgery to remove adhesions and estrogen therapy have been adopted for the treatment of endometrial fibrosis<sup>[5,6]</sup>. However, in severe cases, treatment is difficult and the prognosis is usually suboptimal<sup>[7]</sup>. Therefore, improving the proliferation and regeneration of endometrial epithelium and stromal cells, which in turn can reconstruct the endometrial structure and restore endometrial functioning, is a radical therapy for endometrial damage meant to improve pregnancy rates<sup>[8]</sup>.

Several studies have demonstrated that bone marrow-derived mesenchymal stem cells (BMSCs), which could facilitate proliferation of endometrial stromal and epithelial cells and accretion of endometrium, and represent potential progenitor cells in the endometrial basal layer directly differentiating into endometrial epithelial cells, have beneficial effects for the treatment of IUA<sup>[7-11]</sup>. However, the local microenvironment of damaged endometrium cannot provide the stable three-dimensional structure and necessary bioactive molecules for stem cells. It has yielded disappointing results for transplantation of BMSCs with respect to survival, attachment, differentiation, and proliferation<sup>[12-14]</sup>. The therapeutic effect of direct injection of BMSCs is currently inadequate<sup>[8,10]</sup>.

Pectin is a natural polymer extracted from the peels of apples and oranges, and has good biocompatibility<sup>[15]</sup>. Pluronic® F-127 is a copolymer of polyethylene oxide (PEO) and polypropylene oxide (PPO) which has been used in FDA approved medical products as a pharmaceutical ingredient and can generate and maintain the desired shape through the thermal sol-gel transition<sup>[16]</sup>. Banks A et al. found that Pectin-Pluronic® F-127 hydrogels with three-dimensional loose network structures are more conducive to cell adhesion and survival; Pectin-Pluronic® F-127 hydrogel as a carrier wrap growth factor can significantly extend the release time of growth factors<sup>[17,18][19]</sup>. The hydrogel can be injected into a uterine cavity which has sustained injury to facilitate clinical operation and endometrial regeneration.

Estrogen, specifically 17  $\beta$ -estradiol (E2), is essential for maintaining the microenvironment of endometrium and stimulates regeneration of the endometrium<sup>[8,11,20]</sup>. In clinical practice, E2 therapy is commonly used as an ancillary treatment in IUA patients<sup>[21]</sup>. However, both oral and systemic administration and delivery show low concentrations of E2 at the injured site of the uterus, which significantly reduces its therapeutic effect. E2 at high levels may increase the risk for thrombosis and malignancy<sup>[22]</sup>, and reduces the receptivity of endometrium<sup>[8,11,20,21]</sup>. In situ administration of E2 has many disadvantages including limited half-life period, rapid diffusion into extracellular fluids, and poor solubility in aqueous solutions<sup>[5]</sup>. The limitations of E2 usage were addressed in this study by encapsulating E2 into W/O/W microspheres to construct pectin-based E2-loaded microcapsules (E2 MPs), which could provide sustained E2 release serving as a long-term reliable source of E2 for endometrial regeneration.

Although it has been recognized that E2 plays an indispensable role in promoting the repair of endometrial injury, its mechanism is not well understood. Previous studies have demonstrated that the proliferative and differential responses of epithelial cells and endometrial stem cells to E2 is mediated by endometrial stromal cells (ESCs), which synthesize and transmit paracrine mediators to surrounding cells under the direction of E2<sup>[11,23,24]</sup>. Exosomes (exos) are considered the biological mediators of intercellular communication, and play an important role in regulating cell proliferation and differentiation<sup>[25]</sup>. Exos, one form of extracellular vesicle with a diameter of about 30-150nm, act as carriers of bioactive proteins, lipid bilayer, and genetic material and transfer them to the surrounding cells in the form of paracrine<sup>[26]</sup>. Zhang et al. found that MSCs could be differentiated in the direction of endometrial epithelial cells when they were co-cultured with ESCs and E2<sup>[11,24,27]</sup>. It has been reported that ESCs also have the capacity to release exos to modify endometrial microenvironments in a paracrine fashion<sup>[28]</sup>. Therefore, we consider that exos derived from ESCs play paracrine roles in endometrial regeneration stimulated by E2, potentially modulating the differentiation of BMSCs.

The objectives of this study were to investigate the beneficial effects of BMSCs/E2 MPs/scaffolding grafts on promoting the recovery of injured endometrium, and to investigate the mechanism of BMSCs and E2 in mouse endometrial regeneration.

## **2. Materials And Methods**

### **2.1. BMSCs isolation and culture**

The animal study was performed in strict accordance with the guidelines of the Animal Care and Use Committee in the Xinhua Affiliated Hospital of Shanghai Jiao Tong University, and was approved by Xinhua Hospital Research Ethics Committee, Shanghai Jiao Tong University School of Medicine (reference number: XHEC-F-NSFC-2018-122). BMSCs were isolated and cultured as previously described<sup>[8]</sup>. In brief, five-week-old female C57BL/6 mice were killed. The femora were isolated and rinsed with phosphate-buffered saline (PBS, Gibco, Grand Island, NY, USA). The marrow cells in the bone cavities were flushed out with Dulbecco's Modified Eagle Medium /Nutrient Mixture F-12 (DMEM/F-12, Gibco, USA). The resultant lavage was passed through 100µm cell strainer (BD Bioscience, San Jose, CA, USA) and centrifuged at 1200 rpm for 4 min, which were then re-suspended in DMEM/F-12 supplemented with 10% fetal bovine serum (FBS, Gibco) and 1% Penicillin-Streptomycin (P/S, Gibco). The isolated cells were seeded in 100 mm Petri dish and maintained at 37°C in a humidified incubator supplied with 5% CO<sub>2</sub>. The non-adherent cells were removed after 72 h of culture. The medium was changed every other day and passage was conducted when cells reached confluence (80-100%). The BMSCs of passage 3-5 were used for the following experiments.

### **2.2. Flow cytometric analysis**

The expressions of cell surface markers on BMSCs were evaluated by flow cytometry. BMSCs were detached from the culture dish using 0.05% trypsin-EDTA (Gibco), centrifuged, rinsed and re-suspended in

PBS at a concentration of  $10^5$  cells/mL. Re-suspended cells were incubated with 5 mL of CD44-FITC antibody (eBioscience, San Diego, CA, USA), CD45-BV510 antibody (eBioscience), CD29-APC antibody (eBioscience) and CD105-PE antibody (eBioscience) in the dark at 4 °C for 30 min. After being washed twice with PBS, cytometric analysis was performed with FACSDiva (Canto, BD Bioscience, San Jose, CA, USA) and data were analyzed with FlowJo software (Tree Star, Ashland, OR, USA) (Supplement figure).

## 2.3. Pectin-based E2-loaded microcapsules fabrication

A double emulsion system (W/O/W) was used to generate the microspheres, as shown in previous publications<sup>[29]</sup> (Figure 1). A solution of 2.5 mL of 10 nM 17 $\beta$ -estradiol (E2, Sigma) in ethanol was added to 7.5 mL of pre-warmed 13.33% (w/v) gelatin (Sigma, St. Louis, MO, USA). The first emulsion of gelatin sphere-in-oil (W/O) phase was prepared by adding 1 mL of E2-gelatin solution into 18 mL of pre-warmed (45 °C) olive oil containing 0.5 mL Tween20 (Sigma) and 0.5 mL Span80 (Sigma) as stabilizers. The W/O solution was stirred at 450 rpm for 20 minutes at room temperature to allow for cooling resulting in gelation of the gelatin to produce W/O emulsion. Then, 0.77 mL of the W/O emulsion was added dropwise to 22.23 mL of 3.25% (w/v) low-methoxyl pectin (WillPowder, Miami Beach, FL, USA) solution stirred at 550 rpm to form the double emulsion (W/O/W). An electro-spray set-up (designed by the University of Shanghai for Science and Technology, Shanghai, China) was then used to spray the W/O/W solution into a 0.15 M CaCl<sub>2</sub> solution to induce pectin gelation forming hydrogel microspheres. Pectin-based E2-loaded Microspheres (E2 MPs) were collected through centrifugation and incubated in 50 kD chitosan (Zhejiang Golden-Shell Pharmaceutical Co. Zhejiang, China) solutions for 10 minutes to form the cationic coating. After rinsing in double-distilled water, the E2 MPs were stored in PBS at 4 °C.

## 2.4. Pectin-Pluronic® F-127 scaffolds fabrication

A mixture composed of 3% pectin (w/v) and 20% (w/v) Pluronic® F-127 (Sigma) was used as the basic solution for constructing the scaffold (stored at 4°C). The  $2 \times 10^7$  cells and E2 MPs were then mixed with 10 mL basic solution at 4 °C of final concentration 0.5 mg/mL to construct the scaffold fluid. The mixtures were transferred into a 10 mL plastic syringe and the matched needle (BD) was attached. The mixtures were dropped slowly onto a petri dish heated at 37 °C. When the temperature reached 37°C, the fluid solidified, due to the thermal sol-gel transition of Pluronic® F-127, forming the hydrogel scaffold.

## 2.5. Pectin-Pluronic® F-127 scaffolds degradation

The scaffold samples with diameter  $11 \pm 0.5$  mm and height  $7 \pm 0.4$  mm were prepared and incubated in DMEM/F12 with 10% FBS and 1% P/S at 37°C with 5% CO<sub>2</sub> for 14 days and weighed every day to determine its degradation. The degradation rate was determined as weight remaining (ratio %)<sup>[30]</sup>, as given by the following equation:

$$\text{weight remaining (\%)} = W_a / W_b \times 100$$

where  $W_a$  is the dry gel weight after degradation at different time intervals and  $W_b$  is the dry gel weight before the start of degradation experiment.

The morphology of the lyophilized gel was examined via scanning electron microscopy (SEM). The scaffolds were immersed in liquid nitrogen and lyophilized at room temperature. The cross-section of the hydrogels was gold-coated and viewed using a microscope (PHENOM, Eindhoven, Netherlands).

## **2.6. Enzyme-linked immunosorbent assay for E2 detection**

E2 MPs/scaffolds/BMSCs were cultured in DMEM/F-12 with 10% FBS and 1% P/S and maintained at 37°C with 5% CO<sub>2</sub>. Medium was sampled very day in first 10 days and every other day after that and stored at - 80 °C for further analysis. The concentration of E2 released from microcapsules was measured using an E2 enzyme-linked immunosorbent assay (ELISA) kit (LDN, Nordhorn, Germany) according to the manufacturer's protocols. In brief, indicated medium was centrifuged to remove cell debris. 25 µL of supernatant was dispense into each 96-well plate, which then underwent 1 h of incubation at room temperature on a plate shaker. After adding 100 µL of enzyme conjugate, the plate was incubated for 1h at room temperature on a plate shaker. After complete aspiration of the content, wells were thoroughly washed for four times. After adding 200 µL of substrate solution into each well, the reaction underwent 30 min incubation in dark, and 50 µL stop solution was used to terminate the reaction. TECAN Infinite 200 PRO (TECAN, USA) was used to record absorbance at 450 nm with OD 570 nm as the reference.

## **2.7. Acridine orange/ethidium bromide double fluorescence staining for cell viability determination and imaging**

The BMSCs were incubated with E2-loaded microcapsules in DMEM/F-12 with 10% FBS and 1% P/S for 2 h at 37 °C, using 6-well ultralow attachment plates. The cells and microcapsules were then mixed with Pectin-Pluronic® F-127 solution at 4 °C of final concentration 0.5 mg/mL. The mixtures were transferred into a 10 mL plastic syringe and the matched needle was attached. The mixtures were dropped slowly onto a petri dish heated at 37 °C. After the mixtures formed the scaffolds, 1 mL of pre-warmed medium was added into each well. Cell viability was evaluated on day 7. Equal amounts of 100 µg/mL acridine orange (Sigma) and 100 µg/mL ethidium bromide (Sigma) were used to prepare the AO/EB dye. The AO/EB dye was added into the medium at the ratio of 1:25, and the cells were observed by a fluorescence microscope (Olympus, Tokyo, Japan) after 15 minutes.

## **2.8. Mouse model of endometrial injury and treatment**

In total, 72 nine-week-old females C57BL/6 mice with average body weight 25-30 g were randomly and equally divided into six groups: sham-operated group, spontaneous repair group, BMSCs group, E2/BMSCs group, E2 MPs/BMSCs group, E2 MPs/scaffolds/BMSCs group. For estrous cycle studies, vaginal smears were obtained daily between 8:00-10:00 AM. Only rats with four consecutive 4-day estrus cycles were selected for study. To establish uterine horn damage model, the mice were first anaesthetized, and the skin was sterilized with 10% povidone-iodine. The uterine horns were exposed using a low

abdominal midline incision. After the distal ends of the bilateral uterine horns near the ovaries were incised, an 18 G stainless steel needle with manually grinding rough surface was used to enter the uterine cavity from the incision of the uterine horn and scraped the endometrium repeatedly towards the cervix until the uterine horns were obviously congested. The opened skin and uterine horn were sutured using absorbable suture. The 0.1-0.2mL BMSCs with or without E2 MPs and scaffolds solution were injected into and filled uterine cavity. For spontaneous repair, the uterine horns after modeling were allowed healing without further treatments. For sham operation, after exposure by an abdominal midline incision, the uterine horns were left intact in the abdominal cavity without scratch. All animals were intramuscularly administrated with penicillin twice a day for three consecutive days after surgery to prevent systematic infection.

## 2.9. Histological analysis

The uterine horn at 4 weeks postoperatively was fixed with 4% paraformaldehyde overnight, dehydrated in graded alcohols and embedded in paraffin. Sections of 5  $\mu\text{m}$  were prepared transversally and stained with Hematoxyline-eosin (HE) and Masson staining. For immunohistochemistry, tissue sections were immunolabeled with anti-von Willebrand factor antibody (vWF, Abcam, Cambridge, MA). The thickness of the cross-sectional area of the uterus containing endometrium was quantified. The percentage of the endometrium containing fibrosis, overall endometrium of total epitheliums and secretory glands content in stroma part, total capillary vessels quantity was all semi-quantified using the Image-Pro Plus software.

## 2.10. Functional testing of uterine horns

The function of the regenerated uterine horns was assessed by testing whether it was receptive to a fertilized ovum and whether embryo development was supported to the late stages of pregnancy. Four weeks after the procedure, 6 female mice per group were mated with 2 male C57BL/6 mice. The impregnated mice were euthanized at gestation day 15-19 after the presence of a vaginal plug, and uterine horns were examined for the presence of embryos.

## 2.11. ESCs isolation and culture

Isolation of ESCs was based on the protocol in a previous report<sup>[31]</sup>. Five-week-old female C57BL/6 mice were injected subcutaneously with 100  $\mu\text{L}$  of the E2 solution (100 ng/100  $\mu\text{L}$ ) for 3 consecutive days to stimulate the proliferation of endometrium and killed on the fourth day. The uterine horns were isolated. Uterine horns were transferred to the 0.25% Trypsin-EDTA (Gibco) for 60 min at 4°C, and then incubated for 30 min at 37°C. After incubation, uteri were transfer into a petri dish containing cold DMEM/F12 medium to inactivate trypsin activity, and then vortex for 20 s to release the epithelial sheets. The uteri were transferred to 1mg/mL collagenase I (Sangon Biotech, Shanghai, China) for 30 min at 37°C while shaking (200 rpm). After inhibiting collagenase activity, the stromal cell suspension were centrifuged at 500 x g for 7 min. Cells were re-suspended in DMEM/F-12 with 10% FBS and 1% P/S and then plated on culture dish maintained at 37°C with 5% CO<sub>2</sub>. The non-adherent cells were removed after 6 h of culture.

The medium was changed every other day and passage was conducted when cells reached confluence (80-100%).

## **2.12. Immunofluorescent staining**

Endometrial cells were fixed with 4% paraformaldehyde for 15 min at 4°C and permeabilized with 0.3% Triton X-100 for 1 h at room temperature. They were then incubated at 4 °C overnight with primary antibodies including vimentin (Vim, Abcam) and wide spectrum cytokeratin (Pan-CKs, Abcam). The next day, cells were stained with anti-rabbit IgG-FITC and anti-rabbit IgG-PE secondary antibody (Abcam). Cells were then counterstained with 1 µg/mL DAPI (4,6-diamidino-2-phenylindole; Sigma) for 5 min and observed with a fluorescence microscope (Olympus).

## **2.13. Differentiation of BMSCs into EEC-like cells by co-culture system**

BMSCs and ESCs were co-cultured in Transwell system (12 mm Transwell with a 0.4-µm pore polycarbonate membrane insert, Corning)<sup>[24]</sup>. In brief, BMSCs were seeded in the bottom of six-well plate at a density of  $6 \times 10^5$  cells/well and ESCs were seeded on the Transwell membrane at a density of  $6 \times 10^4$  cells/well to separate the cells but allow soluble factors to pass freely between them. Six experimental groups were set up. In group A (control group), BMSCs were cultured in the bottom of the co-culture system alone without ESCs in differentiation medium (DMEM/F-12 with 2% Charcoal-Stripped FBS, BI, USA); in groups B, C, D, E, and F, BMSCs were co-cultured with ESCs and different concentrations of E2 (0, 1, 10, 100, 1000 nM, respectively) in differentiation medium. The medium was changed every two days over a period of 4 weeks.

## **2.14. Western blot analysis**

Differentiated BMSCs and exosomes were lysed in RIPA buffer (Beyotime, Shanghai, China). The protein in the supernatant was quantified using the BCA Protein Assay Kit (Thermo Scientific™, USA), electrophoresed on a 12% SDS-PAGE gel, and transferred to polyvinylidene fluoride membrane (PVDF, Millipore, Billerica, MA). After blocking, the membranes were incubated at 4 °C overnight with one of the following antibodies: CD9 (Abcam), Tsg101 (Abcam), CD63 (Abcam), PR (Invitrogen, Waltham, MA, USA), ER-α (Invitrogen), CK19 (Novus, Littleton, USA), CK18 (Abclonal, Wuhan, China), CK13 (ABclonal), β-actin (Cell Signaling Technology, Danvers, MA, USA), or GAPDH (Cell Signaling Technology). Anti-rabbit IgG, HRP-linked antibody (Cell Signaling Technology) and anti-mouse IgG, HRP-linked antibody (Cell Signaling Technology) were used as the secondary antibodies. The labeled proteins were visualized with the ChemiDoc™ XRS imaging system (Bio-Rad Laboratories, Inc., Hercules, CA, USA) using an enhanced chemiluminescence (ECL) kit (Pierce). ImageJ software was used for Western blot grayscale analysis.

## **2.15. Exosome isolation**

ESCs at 70% of confluence were incubated in DMEM/F12 containing 10% exosome-depleted FBS (System Biosciences, CA, USA) for 48 h. Subsequently, the medium of ESCs was collected and

centrifuged at 2000 g for 10 min at 4 °C to eliminate cell debris. The resulting supernatants were filtered through a 0.22- $\mu$ m filter (Millipore, Billerica, MA, USA) to remove microvesicles, and then concentrated through an Amicon Ultra-15 100 kDa centrifugal filter (Millipore, Billerica, MA, USA) at 4000 rpm for 30 min. Exosomes were then isolated using the Total Exosome Isolation kit (Invitrogen, Carlsbad, CA, USA) according to the manufacturer's protocol. Briefly, the supernatant was mixed with Total Exosome Reagent and incubated for 24 h at 4°C. Samples were centrifuged at 10,000 x g for 2 h and the supernatant removed. The exosome pellet was re-suspended in 100  $\mu$ L of PBS and stored at -80 °C.

### **2.16. Identification of ESCs-derived exosomes**

The size distribution of ESCs-derived exosomes (ESCs-Exos) was measured by nanoparticle tracking analysis (NTA) with a NanoSight NS3000 instrument (Malvern Instruments, Malvern, UK), and the exosomes morphologies were observed by transmission electron microscope (Hitachi, Tokyo, Japan). The characteristic surface marker proteins of exosomes were analyzed by Western blot.

### **2.17. Exosome uptake**

Exosomes were labeled with a membrane-labeling dye (1,1'-Dioctadecyl-3,3,3',3'-Tetramethylindocarbocyanine Perchlorate, Dil) according to the manufacturer's protocol (Invitrogen). Briefly, 15  $\mu$ g exosomes diluted in DMEM/F12 medium were added to 0.5  $\mu$ L Dil and incubated for 20 min at 37°C with 5% CO<sub>2</sub>. Excess dye was removed from the labeled exosomes by ultracentrifugation at 100,000 g for 70 min at 4 °C, and the exosome pellets were purified on Exosome Spin Columns MW 3000 (Invitrogen) according to the manufacturer's instructions. The final pellets were re-suspended in 100  $\mu$ L PBS. Dil-Labelled exosomes were added to the culture medium of BMSCs, which were seeded at a density of 250 cells/mm<sup>2</sup> the previous day and incubated at 37°C for 2 h. Subsequently, BMSCs were fixed with 4% paraformaldehyde for 15 min at 4°C, and then counterstained with 1  $\mu$ g/mL DAPI for 5 min. The fluorescence was detected under a confocal laser scanning microscope (Leica TCS SP8, Leica Microsystems, Buffalo Grove, IL, USA). At last, co-localization was performed using the Image J Fiji software.

### **2.18. Exosome mediated stem cell differentiation**

BMSCs were plated at a density of 150 cells/mm<sup>2</sup>. After 24 h, BMSCs were rinsed with PBS and then maintained in a differentiation medium, differentiation medium containing ESCs-Exos with 50  $\mu$ g/mL, or differentiation medium containing exosomes released from ESCs by E2 stimulation (E2-ESCs-Exos) with 50  $\mu$ g/mL. The medium was changed every 2 days for up to 4 weeks.

### **2.19. Statistical analysis**

All data in this study were analyzed with SPSS 23.0 and presented as mean  $\pm$  SD. Significance of difference between two groups was tested by Student's t-test or ANOVA. Fisher's exact test (Freeman-Halton) was employed to assess the outcome of treatment.  $\chi^2$  tests were performed to compare

pregnancy rates. The statistical significances were presented as  $p$  values, and  $p < 0.05$  was considered statistically significant.

## 3. Results

### 3.1. Fabrication and characterization of Pectin-Pluronic® F-127 scaffolds

When temperature increases from below to above (37 °C for this study) its lower critical solution temperature (LCST), Pluronic® F-127 with a sol-gel transition behavior in aqueous solution can help generate and maintain the desired shape. Figure 2A shows the images of the Pectin-Pluronic® F-127 solution (Left) and scaffolds (Right). Then, BMSCs were suspended in Pectin-Pluronic® F-127 solution to reach a  $1 \times 10^6$  cells/mL concentration for forming the scaffolds. As revealed in the SEM images, Pectin-Pluronic® F-127 scaffolds exhibit uniform pores with a mean diameter of 150~400  $\mu\text{m}$ , which indicates excellent water absorption capacity and a fair improvement in the three-dimensional network structure of the Pectin-Pluronic® F-127 scaffolds (Figure 2B). These continuously interconnected porous structures are also conducive to the nutrient supply for cell growth in tissue engineering. BMSCs could attached to the scaffold and distributed the inner space of the scaffold (Figure 2C). As shown in Figure 2D, the scaffold began to degrade after day 5, and approximately 28% of scaffold degraded at a consistent and sustained pace at day 14.

The cytotoxicity of scaffolds was further explored. After 7 days of culture, the even distribution of BMSCs within the scaffold can be viewed in focus and out of focus as they are at different planes by AO/EB staining (Figure 2E). BMSCs had a high cellular viability rate of  $95.98 \pm 1.30\%$  within the bioprinted scaffold compared to  $98.00 \pm 0.50\%$  for control, indicating that the scaffold could provide 3D architecture for the attachment of BMSCs and exhibit negligible toxicity of BMSCs for the culture *in vitro* ( $p=0.0656$ ) (Figure 2E and F).

### 3.2. Preparation and characterization of Pectin-based E2-loaded microcapsules

Figure 3A and B present that the double emulsion (W/O/W) microspheres were successfully created with the diameters averaging around 100  $\mu\text{m}$ . Then, BMSCs were co-incubated with E2 MPs for 72 h. The cell counting kit-8 assay revealed that BMSCs incubated with E2 MPs proliferated faster than those without E2 MPs (Figure 3C). Furthermore, Pectin-based E2-loaded microcapsules (E2 MPs) (equivalent concentration 10 nM) were incubated in medium, which was harvested for 30 days to assay for the release of E2 using ELISA. As shown in Figure 3D, the E2 in medium would degrade rapidly, and the effective concentration of E2 was reduced to 19.7% of the original concentration in the first 24 h and almost completely degraded within 72 h. However, the microcapsule could maintain the effective concentration of E2 in medium for 30 days by controlling the release of E2. These results supported that

E2 was shown to be successfully encapsulated into the W/O/W microspheres, which provided a sustained E2 release and served as a reliable source of E2 to promote endometrial regeneration.

The prepared E2 MPs and BMSCs were mixed with Pectin-Pluronic® F-127 solution to generate the hydrogel scaffold for investigating the influence of E2 MPs on micro-vascularized 3D tissue formation. The presence of the W/O/W microspheres does not impact the scaffold formation process. Without microcapsule, the BMSCs are evenly distributed within the scaffolds. In the presence of E2 MPs, the BMSCs self-assembled around the E2 MPs and interacted to form a three-dimensional network (Figure 3E).

### **3.4. BMSCs/E2 MPs/scaffolds system for *in vivo* endometrial regeneration in mice**

To investigate the potential therapeutic effect of BMSCs/E2 MPs/scaffolds transplantation in endometrial regeneration, BMSCs/E2 MPs/scaffolds were injected into the uterine cavity of mouse endometrial injury model. At 28 days after surgery, E2 MPs and scaffolds were completely degraded. Sections of all groups were lined by simple columnar epitheliums that were similar to the Sham group. Endometrial tissue in BMSCs/E2 MPs/scaffolds group appeared well organized with epitheliums, secretory glands and apparent neovascularization, while endometrial of spontaneous regeneration group formed the scar tissues with collagen deposition (Figure 4). The thickness of endometrial in BMSCs/E2 MPs/scaffolds ( $877.95 \pm 23.95 \mu\text{m}$ ) was similar to that in sham group ( $896.41 \pm 62.65 \mu\text{m}$ ) and was higher than the spontaneous group ( $574.87 \pm 149.43 \mu\text{m}$ ), BMSCs group ( $612.78 \pm 29.05 \mu\text{m}$ ), BMSCs/E2 groups ( $723.89 \pm 108.75 \mu\text{m}$ ) and BMSCs/Scaffolds groups ( $728.78 \pm 111.75 \mu\text{m}$ ) ( $p < 0.05$ , respectively) (Figure 4A and B). In addition, although the rate of endometrial fibrosis in mice receiving BMSCs/E2 MPs/scaffolds ( $0.27 \pm 0.11\%$ ) was slightly higher than in the sham operated group ( $0.23 \pm 0.07\%$ ), it was significantly lower than in the spontaneous regeneration group ( $4.26 \pm 2.65\%$ ), the group receiving BMSCs alone ( $2.71 \pm 1.24\%$ ) and the group receiving BMSCs/E2 ( $2.26 \pm 1.50\%$ ) ( $p < 0.05$ ) (Figure 4C and D).

Neovascularization in regenerating endometrium is important for the restoration of functional fertility. At 28 days, blood vessel density in the endometrial tissue after implantation of BMSCs/E2 MPs/scaffolds grafts ( $11.3 \pm 2.9$ ) was significantly higher than that in spontaneous group ( $3 \pm 2.2$ ), BMSCs group ( $5.5 \pm 2.1$ ), BMSCs/E2 group ( $6 \pm 1.4$ ) and ( $p < 0.05$ , respectively) ( $p < 0.05$ ), while still comparable to that in BMSCs/Scaffolds group ( $8.8 \pm 2.8$ ) and sham operated group ( $10 \pm 2.2$ ) (Figure 4E, F and G).

#### **3.4.3 Pregnancy within the regenerated uterine horns**

Four weeks after surgery, pregnancy was observed in some of the regenerated uterine horns, which were maintained to a late, viable stage of pregnancy. Implanted embryos were present in some of the regenerated uteri after grafting with BMSCs, BMSCs with E2 or scaffolds, but embryos were found in all regenerated uterine horns in BMSCs/E2 MPs/scaffolds group. The pregnancy rate of BMSCs/E2 MPs/scaffolds group (100%) was much higher than those of spontaneous regeneration group (25%),

BMSCs group (41.7%), BMSCs/E2 group (50%), BMSCs/scaffolds group (66.7%), and comparable with that of sham operated group (100%) (Figure 5). This suggested a nearly full uterine recovery from injury in pregnancy rate. These results supported the beneficial effect of BMSCs/E2 MPs/scaffolds in promoting the recovery of injured endometrium to functional endometrium.

### **3.5. Culture and identification of endometrial cells**

Endometrial cells were isolated from mice. ESCs were spindle-shaped fibroblast-like cells, while EECs were polygonal cells rounder than stromal cells (Figure 6A). A vimentin/cytokeratin double staining was performed and indicated that stromal cells were positive for vimentin (Vim), and negative for cytokeratin (Pan-CKs), whereas epithelial cells do express Pan-CKs but not Vim. These immunofluorescence staining showed that endometrial stromal cell culture has a purity of up to 90% (Figure 6B).

### **3.6. Evaluation of the effects of E2 on epithelial differentiation of BMSCs**

BMSCs were co-cultured with ESCs in Transwell system, the system is characterized by separating the cells but allowing soluble factors to pass freely between them. After 6 weeks of culture, the expression of endometrial epithelial cell markers, CK19, CK18, CK13, ER- $\alpha$  and PR on BMSCs were tested by Western blot. Notably, these markers expression were up-regulated in BMSCs co-cultured with ESCs compared to that in BMSCs cultured alone (Figure. 6C). This suggests that endogenous factors secreted by ESCs provide an environment for BMSCs to differentiate in the direction of epithelial cells.

Then, BMSCs were treated with gradient concentrations of E2 (0, 1, 10, 100, 1000 nM, respectively) in the co-culture system. A Western blot showed that E2 dose-dependently promoted BMSCs differentiation. After 6 weeks in culture, the expression levels of the endometrial epithelial cell markers except ER- $\alpha$  were highest in cells cultured with  $1 \times 10^{-8}$  mol/L E2 ( $p < 0.05$ ). This data suggested that 10 nM E2 provided the optimal microenvironment for the differentiation of BMSCs towards epithelial lineages (Figure 6D).

### **3.7. Characterization of ESCs-Exos**

Exosomes derived from ESCs (ESCs-Exos) were characterized in terms of size, morphology, and surface markers. NTA revealed that the diameters of these particles predominantly ranged from 30 nm to 150 nm (Figure 7A). ESCs-Exos exhibited a cup- or sphere-shaped morphology (Figure 7B), as shown by TEM. The identity of these particles was further confirmed as exosomes by Western blot, which showed the presence of exosomal surface markers including CD63, CD9 and TSG101 (Figure 7C). All this data suggested that these nanoparticles were indeed exosomes.

### **3.8. Responses of BMSCs to ESCs-Exos *in vitro***

The confocal microscope observed that exosomes were internalized into the cytoplasm of BMSCs and were partly co-localized within the nuclei (Figure 7D), which implied that ESCs-Exos can be transferred into stem cells with high cellular uptake efficiency. Furthermore, BMSCs were co-incubated with exosomes released from ESCs with or without E2 stimulation. After 21 days of culture, the expression of

the endometrial epithelial cell markers, CK19, CK18, CK13, ER- $\alpha$  and PR significantly augmented in BMSCs treated with 50  $\mu\text{g}/\text{mL}$  of ESCs-Exos. However, exosomes derived from E2-stimulated ESCs (E2-ESCs-Exos) could further promote the expression level of these markers in BMSCs (Figure 8A). Higher proportion of Pan-CKs staining positive cells were also observed in this group according to immunofluorescence analysis (Figure 8B). These results indicated that ESCs-Exos provided biochemical cues to stimulate differentiation of BMSCs towards endometrial epithelial cells, and involvement of E2 could enhance its differentiation-promoting capacity.

## 4. Discussion

Intrauterine adhesions (IUA) frequently occur after infectious or mechanical injury to the endometrium, which may lead to infertility and/or pregnancy complications<sup>[3,4]</sup>. Several strategies, such as hysteroscopic surgery to remove adhesions and hormonal therapy have been adopted for the treatment of endometrial fibrosis<sup>[5,6]</sup>. However, due to severe damages to the basilar layer results in loss of resident stem cells and injures the microenvironment of endometrium followed by the failure of endometrial functional layer regeneration<sup>[3,4]</sup>, treatment in severe cases is difficult and the prognosis is usually suboptimal<sup>[7]</sup>. BMSCs have been recognized as new candidates for treating serious endometrial injuries<sup>[32,33]</sup>. However, low differentiation efficiency and poor proliferation ability remain as the major hurdles BMSCs transplantation<sup>[7,8,10]</sup>. Thus, a therapeutic strategy, by modifying endometrial microenvironment with promotion of BMSCs survival, attachment, proliferation and differentiation, is needed for the restoration of endometrium.

Both Pectin and Pluronic® F-127 show well-proved biocompatibility and bioactivity<sup>[15]</sup>. In addition, Pluronic® F-127 exhibits a sol-gel transition behavior in aqueous solution when temperature increases from below to above (37 °C used in this study) its lower critical solution temperature<sup>[16]</sup>. Thus, the Pectin-Pluronic® F-127 solution can completely fill the uterine cavity and reach the injured region and form the hydrogel scaffold *in vivo*. In the present study, it was found that a Pectin-Pluronic® F-127 hydrogel with slow degradation time and three-dimensional loose network structure is more conducive to BMSCs adhesion and survival. The low degradation rate promotes their applications for long-term delivery. BMSCs/Scaffolds group shows better integration into adjacent tissues and more effective tissue regeneration at 4 weeks after surgery than BMSCs groups, such as marked proliferation of cells and abundant neovascularization.

E2 is essential for maintaining the microenvironment of endometrium. In clinical practice, E2 therapy after adhesiolysis is considered an effective ancillary treatment to restore endometrium function for IUA patients<sup>[21]</sup>. Based on our and other previous studies, E2 is responsible for uterine endometrial regeneration through stimulating the proliferation and differentiation of stem cells and forming new capillaries after injury<sup>[8,11,20]</sup>. However, the usage of E2 is limited by its low concentration at the injured uterus, the risk for thrombosis and malignancy in systemic administration, a limited half-life period, rapid diffusion into extracellular fluids, and poor solubility in aqueous solutions. Hence, it is challenging to

retain E2 at the injured endometrium when administered through simple injections<sup>[8,11,20,21]</sup>. The aim of this study was to develop a new sustained release system intended for the *in situ* administration of E2. In this project, E2 was encapsulated into the W/O/W microspheres to construct Pectin-based E2-loaded microcapsules (E2 MPs), which could maintain the effective concentration of E2 in the medium within 30 days by the controlled release E2 to promote the differentiation of BMSCs and endometrial regeneration. The therapeutic effect of BMSCs/E2 MPs/scaffolds group in promoting recovery of functional endometrium was also proven. At four weeks after the transplantation, BMSCs/E2 MPs/scaffolds system increased proliferative abilities of uterine endometrial and vascular endothelial cell. Furthermore, Zhang et al. demonstrated the potential of microsphere incorporated scaffolds for generating vascularized tissue when co-incubated with HUVECs, which self-assembled around the MPs and formed a 3D vascular-like network<sup>[34]</sup>. In our mouse endometrial injury model, the BMSCs/E2 MPs/scaffolds group also showed an increased expression of the blood vessel marker vWF and more vessels within regenerated endometrium. BMSCs/E2 MPs/scaffolds that promoted restoration of the endometrial construction may, to some extent, have resulted from increased vascularity that improves the access to nutrients, oxygen and hormones of injured tissues. Pregnancy rate of the BMSCs/E2 MPs/scaffolds group after the transplantation was significantly higher than other groups, indicating well developed endometrial glands, uterine vasculature, and a normal reproductive hormone response of the regenerated tissue in the BMSCs/E2 MPs/scaffolds group, close to normal tissue. Therefore, BMSCs/E2 MPs/scaffolds system is a promising strategy for endometrial tissue regeneration.

Although it has been recognized that E2 plays an indispensable role in promoting the repair of endometrial injury, its mechanism remains poorly understood. Based on previous studies, the proliferative and differential response of epithelial cells and endometrial stem cells to E2 is mediated by endometrial stromal cells (ESCs), which synthesize and transmit paracrine mediators to surrounding cells under the direction of E2<sup>[23,24,35]</sup>. In the present study, BMSCs were co-cultured with ESCs in Transwell system. After 6 weeks of culture, the expression of endometrial epithelial cell markers was up-regulated in BMSCs co-cultured with ESCs, and E2 is an effective inducer for facilitating the differentiation of BMSCs towards epithelial lineages. It has been noted that the exogenous stem cells implanted into the endometrium are surrounded by endometrial stroma which provides a local environment for BMSC survival and motivates cell differentiation in the direction of epithelial cells to reconstruct the injured uterine endometrium via the autocrine and paracrine pathways<sup>[36]</sup>. Several studies reported that endometrial stromal cells can secrete a large number of vesicles, i.e., exosomes, that influence the growth, function, and development of endometrial tissue<sup>[37-41]</sup>. Exosomes, which act as carriers of bioactive proteins, lipid bilayer and genetic material, are considered the biological mediator of intercellular communication and play a key role in regulating cell proliferation and differentiation<sup>[25,26,42,43]</sup>. In the present study, we found that ESCs could secrete exosomes, which are successfully delivered into BMSCs with high cellular uptake efficiency and significantly affect cell proliferation in a dose-dependent manner. ESCs-derived exosomes provide biochemical cues to direct differentiation of BMSCs towards endometrial epithelium, and their functional effects were more significant than that of ESCs itself. In addition, exosomes derived from E2-stimulated ESCs could enhance the differentiation efficiency of BMSCs. These results suggest that exosomes

derived from ESCs play paracrine roles in endometrial regeneration stimulated by E2 through inducing the differentiation of BMSCs into endometrial epithelial cells.

## 5. Conclusion

The BMSCs/E2 MPs/scaffolds therapeutic strategy may be beneficial in the treatment of severely damaged endometrium. The BMSCs/E2 MPs/scaffolds system could provide a three-dimensional architecture for the attachment, growth and migration of BMSCs and vascularization promotion, while serving as a reliable source of E2 to promote endometrial regeneration. Furthermore, exosomes derived from ESCs play paracrine roles in endometrial regeneration stimulated by E2, potentially modulating the differentiation of BMSCs.

## Abbreviations

BMSCs: Bone marrow-derived mesenchymal stem cells; E2 MPs: Pectin-based E2-loaded microcapsules; EECs: Endometrial epithelial cells; ESCs: Endometrial stromal cells; Exos: Exosomes; ESCs-Exos: Exosomes secreted from endometrial stromal cells; E2-ESCs-Exos: Exosomes derived from E2-stimulated ESCs; IUA: intrauterine adhesion; E2: 17  $\beta$ -estradiol; PEO: polyethylene oxide; PPO: polypropylene oxide; PBS: phosphate-buffered saline; DMEM/F-12: Dulbecco's Modified Eagle Medium /Nutrient Mixture F-12; FBS: fetal bovine serum; P/S: Penicillin-Streptomycin; ELISA: enzyme-linked immunosorbent assay; vWF: von Willebrand factor; HE: Hematoxyline-eosin; Vim: Vimentin; Pan-CKs: Wide spectrum cytokeratin; NTA: Nanoparticle tracking analysis; LCST: Lower critical solution temperature;

## Declarations

### Acknowledgements

The authors would like to thank Gina Mazzone (MSOE) for proofreading the manuscript.

### Authors' contributions

YW and SG performed experiments. YW and SG performed the data analysis. YW, SG, JMC, GHD, TAM and CJS contributed to data interpretation. BL, WZ and XH designed experiments. YW and SG wrote the manuscript. JMC, GHD, TAM and CJS helped make critical revisions to the manuscript. All authors have read and approved the final manuscript.

### Funding

This research was supported by a research grant (81873816) from the National Natural Science Foundation of China.

### Availability of data and materials

The data that support the findings of this study are available from the corresponding author upon reasonable request.

### **Ethics approval and consent to participate**

All animal studies were conducted under a protocol approved by Xinhua Hospital Research Ethics Committee, Shanghai Jiao Tong University School of Medicine (reference number: XHEC-F-NSFC-2018-122).

### **Consent for publication**

Not applicable.

### **Competing interest**

The authors declare that they have no known competing financial interests or personal relationships that may have influenced the work reported in this paper.

### **Author details**

<sup>1</sup>Shanghai Key Laboratory of Maternal Fetal Medicine, Shanghai First Maternity and Infant Hospital, School of Medicine, Tongji University, Shanghai, 200092, China. <sup>2</sup>Obstetrics Department, Shanghai First Maternity and Infant Hospital, School of Medicine, Tongji University, Shanghai, 200092, China. <sup>3</sup>Biomolecular Engineering Program, Department of Physics and Chemistry, Milwaukee School of Engineering, Milwaukee WI 53202, USA. <sup>4</sup>School of Medical Instrument and Food Engineering, University of Shanghai for Science and Technology, Shanghai 200093, China

## **References**

1. Evans J, Salamonsen LA, Winship A, et al. Fertile ground: human endometrial programming and lessons in health and disease. *Nat Rev Endocrinol.* **2016**, *12*. 11, 654-667.
2. Gargett CE, Schwab KE, Deane JA. Endometrial stem/progenitor cells: the first 10 years. *Human Reproduction Update.* **2015**. dmv051.
3. Maybin JA, Critchley HOD. Menstrual physiology: implications for endometrial pathology and beyond. *Human Reproduction Update.* **2015**, *21*. 6, 748-761.
4. Tuuli MG, Shanks A, Bernhard L, et al. Uterine synechiae and pregnancy complications. *Obstet Gynecol.* **2012**, *119*. 4, 810-814.
5. Yu D, Wong YM, Cheong Y, et al. Asherman syndrome—one century later. *Fertil Steril.* **2008**, *89*. 4, 759-779.
6. March CM. Management of Asherman's syndrome. *Reprod Biomed Online.* **2011**, *23*. 1, 63-76.

7. Jing Z, Qiong Z, Yonggang W, et al. Rat bone marrow mesenchymal stem cells improve regeneration of thin endometrium in rat. *Fertility and Sterility*. **2014**, *101*. 2, 587-594.e583.
8. Wang L, Yang M, Jin M, et al. Transplant of insulin-like growth factor-1 expressing bone marrow stem cells improves functional regeneration of injured rat uterus by NF-kappaB pathway. *J Cell Mol Med*. **2018**, *22*. 5, 2815-2825.
9. Alawadhi F, Du H, Cakmak H, et al. Bone Marrow-Derived Stem Cell (BMDSC) transplantation improves fertility in a murine model of Asherman's syndrome. *PLoS One*. **2014**, *9*. 5, e96662.
10. Ding L, Li X, Sun H, et al. Transplantation of bone marrow mesenchymal stem cells on collagen scaffolds for the functional regeneration of injured rat uterus. *Biomaterials*. **2014**, *35*. 18, 4888-4900.
11. Zhang WB, Cheng MJ, Huang YT, et al. A study in vitro on differentiation of bone marrow mesenchymal stem cells into endometrial epithelial cells in mice. *Eur J Obstet Gynecol Reprod Biol*. **2012**, *160*. 2, 185-190.
12. Murrow LM, Weber RJ, Gartner ZJ. Dissecting the stem cell niche with organoid models: an engineering-based approach. *Development*. **2017**, *144*. 6, 998-1007.
13. Chacon-Martinez CA, Koester J, Wickstrom SA. Signaling in the stem cell niche: regulating cell fate, function and plasticity. *Development*. **2018**, *145*. 15.
14. Santamaria X, Mas A, Cervelló I, et al. Uterine stem cells: from basic research to advanced cell therapies. *Human Reproduction Update*. **2018**, *24*. 6, 673-693.
15. Zhang W, Bissen MJ, Savela ES, et al. Design of artificial red blood cells using polymeric hydrogel microcapsules: hydrogel stability improvement and polymer selection. *The International journal of artificial organs*. **2016**. 0.
16. Zhang W, Gilstrap K, Wu L, et al. Synthesis and characterization of thermally responsive Pluronic F127-chitosan nanocapsules for controlled release and intracellular delivery of small molecules. *ACS nano*. **2010**, *4*. 11, 6747-6759.
17. Banks A, Guo X, Chen J, et al. Novel bioprinting method using a pectin based bioink. *Technology and health care : official journal of the European Society for Engineering and Medicine*. **2017**, *25*. 4, 651-655.
18. Crouse JZ, Mahuta KM, Mikulski BA, et al. Development of a microscale red blood cell-shaped pectin-oligochitosan hydrogel system using an electrospray-vibration method: preparation and characterization. *Journal of applied biomaterials & functional materials*. **2015**, *13*. 4, e326-331.
19. Devon McCune, Xiaoru Guo, Tong Shi, Samuel Stealey, Romare Antrobus, Matey Kaltchev, Junhong Chen, Subha Kumpaty, Xiaolin Hua, Weiping Ren, Wujie Zhang. Electrospinning pectin-based nanofibers: a parametric and cross-linker study. APPL NANOSCI. <https://doi.org/10.1007/s13204-018-0649-4>.
20. Fatima LA, Campello RS, Santos RS, et al. Estrogen receptor 1 (ESR1) regulates VEGFA in adipose tissue. *Scientific reports*. **2017**, *7*. 1, 16716.
21. Zhang SS, Xia WT, Xu J, et al. Three-dimensional structure micelles of heparin-ploxamer improve the therapeutic effect of 17beta-estradiol on endometrial regeneration for intrauterine adhesions in a

- rat model. *Int J Nanomedicine*. **2017**, *12*. 5643-5657.
22. Cintron D, Rodriguez-Gutierrez R, Serrano V, et al. Effect of estrogen replacement therapy on bone and cardiovascular outcomes in women with turner syndrome: a systematic review and meta-analysis. *Endocrine*. **2017**, *55*. 2, 366-375.
23. Chung D, Gao F, Jegga AG, et al. Estrogen mediated epithelial proliferation in the uterus is directed by stromal Fgf10 and Bmp8a. *Mol Cell Endocrinol*. **2015**, *400*. 48-60.
24. Shi Q, Gao J, Jiang Y, et al. Differentiation of human umbilical cord Wharton's jelly-derived mesenchymal stem cells into endometrial cells. *Stem Cell Res Ther*. **2017**, *8*. 1, 246.
25. Nabariya DK, Pallu R, Yenuganti VR. Exosomes: The protagonists in the tale of colorectal cancer? *Biochim Biophys Acta Rev Cancer*. **2020**, *1874*. 2, 188426.
26. Liu J, Jiang F, Jiang Y, et al. Roles of Exosomes in Ocular Diseases. *Int J Nanomedicine*. **2020**, *15*. 10519-10538.
27. Song T, Zhao X, Sun H, et al. Regeneration of uterine horns in rats using collagen scaffolds loaded with human embryonic stem cell-derived endometrium-like cells. *Tissue Eng Part A*. **2015**, *21*. 1-2, 353-361.
28. Harp D, Driss A, Mehrabi S, et al. Exosomes derived from endometriotic stromal cells have enhanced angiogenic effects in vitro. *Cell Tissue Res*. **2016**, *365*. 1, 187-196.
29. Johnson DL, Ziemba RM, Shebesta JH, et al. Design of pectin-based bioink containing bioactive agent-loaded microspheres for bioprinting. *Biomedical Physics & Engineering Express*. **2019**, *5*. 6.
30. Yan S, Wang T, Li X, et al. Fabrication of injectable hydrogels based on poly(L-glutamic acid) and chitosan. *RSC Advances*. **2017**, *7*. 28, 17005-17019.
31. De CK, Hennes A, Vriens J. Isolation of Mouse Endometrial Epithelial and Stromal Cells for In Vitro Decidualization. *Journal of Visualized Experiments Jove*. **2017**, *2017*. 121.
32. Taylor HS. Endometrial cells derived from donor stem cells in bone marrow transplant recipients. *JAMA*. **2004**, *292*. 1, 81-85.
33. Ikoma T, Kyo S, Maida Y, et al. Bone marrow-derived cells from male donors can compose endometrial glands in female transplant recipients. *Am J Obstet Gynecol*. **2009**, *201*. 6, 608 e601-608.
34. Zhang W, Choi JK, He X. Engineering Microvascularized 3D Tissue Using Alginate-Chitosan Microcapsules. *J Biomater Tissue Eng*. **2017**, *7*. 2, 170-173.
35. Song T, Zhao X, Sun H, et al. Regeneration of Uterine Horns in Rats Using Collagen Scaffolds Loaded with Human Embryonic Stem Cell-Derived Endometrium-Like Cells. *Tissue Engineering Part A*. **2015**, *21*. 1-2, 353-361.
36. Du H, Taylor HS. Contribution of bone marrow-derived stem cells to endometrium and endometriosis. *Stem Cells*. **2007**, *25*. 8, 2082-2086.
37. Wu D, Lu P, Mi X, et al. Exosomal miR-214 from endometrial stromal cells inhibits endometriosis fibrosis. *MHR: Basic science of reproductive medicine*. **2018**.

38. Sun H, Li D, Yuan M, et al. Macrophages alternatively activated by endometriosis-exosomes contribute to the development of lesions in mice. *Mol Hum Reprod.* **2019**, *25*. 1, 5-16.
39. Harp D, Driss A, Mehrabi S, et al. Exosomes derived from endometriotic stromal cells have enhanced angiogenic effects in vitro. *Cell & Tissue Research.* **2016**, *365*. 1, 187-196.
40. Blázquez-Rodríguez S, Sánchez-Margallo FM, Vázquez A, et al. Murine embryos exposed to human endometrial MSCs-derived extracellular vesicles exhibit higher VEGF/PDGF AA release, increased blastomere count and hatching rates. *Plos One.* **2018**, *13*. 4, e0196080.
41. Maida Y, Takakura M, Nishiuchi T, et al. Exosomal transfer of functional small RNAs mediates cancer-stroma communication in human endometrium. *Cancer Med.* **2016**, *5*. 2, 304-314.
42. Kourembanas S. Exosomes: vehicles of intercellular signaling, biomarkers, and vectors of cell therapy. *Annu Rev Physiol.* **2015**, *77*. 13-27.
43. Thery C, Zitvogel L, Amigorena S. Exosomes: composition, biogenesis and function. *Nat Rev Immunol.* **2002**, *2*. 8, 569-579.

## Figures

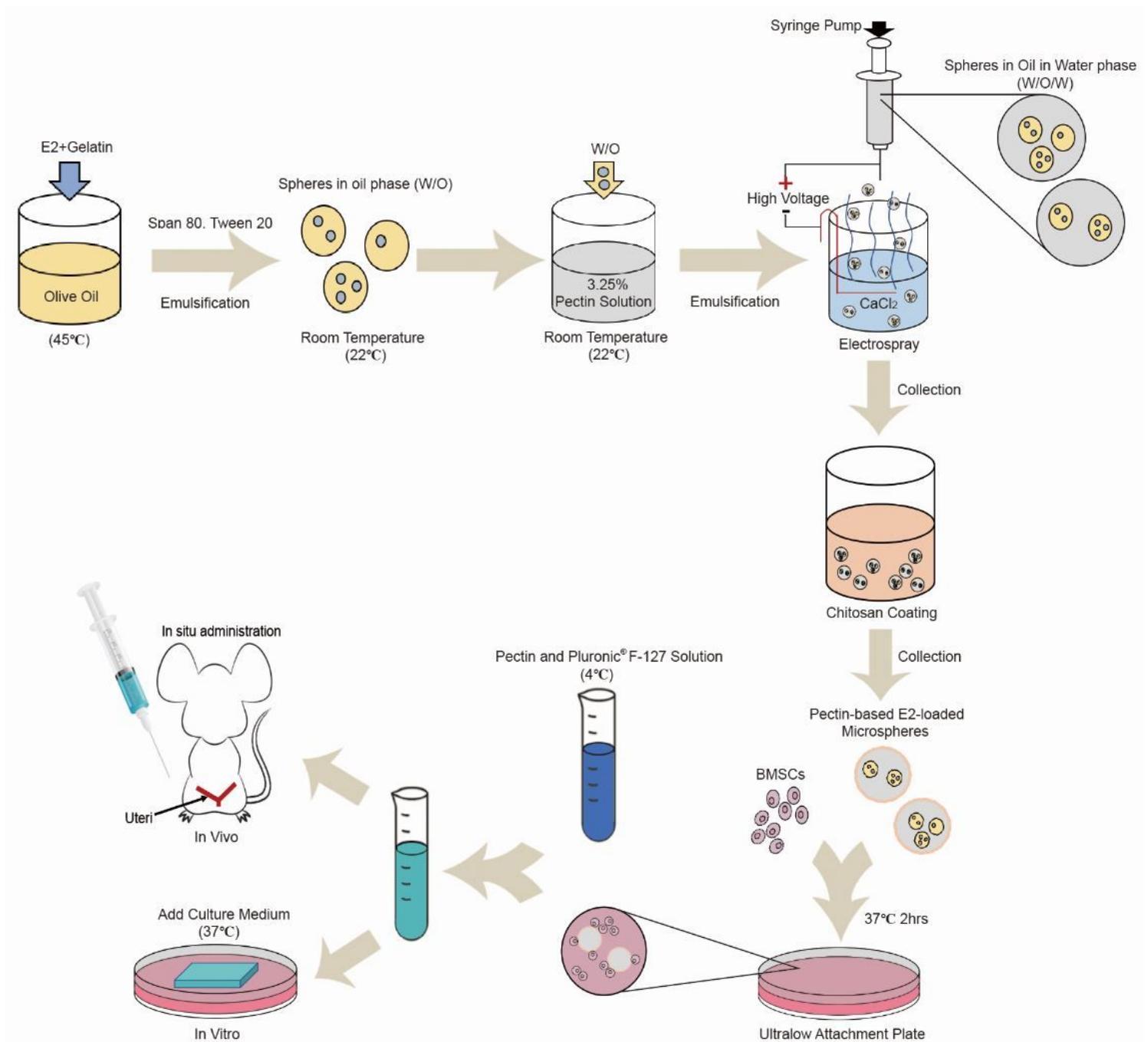


**Figure 1**

A schematic illustration of the procedure for fabricating Pectin-based E2-loaded microcapsules and Pectin-Pluronic® F-127 scaffolds for endometrial regeneration: (1) preparing microsphere by electro-spray and coating with chitosan; (2) incubating Cells with E2-loaded microcapsules; (3) mixing with Pectin-Pluronic® F-127 solution; (4) evaluating the therapeutic effects of E2 MPs composite scaffolds in vitro; (5) evaluating the BMSCs/E2 MPs/scaffolds system for in vivo endometrial regeneration in mice.

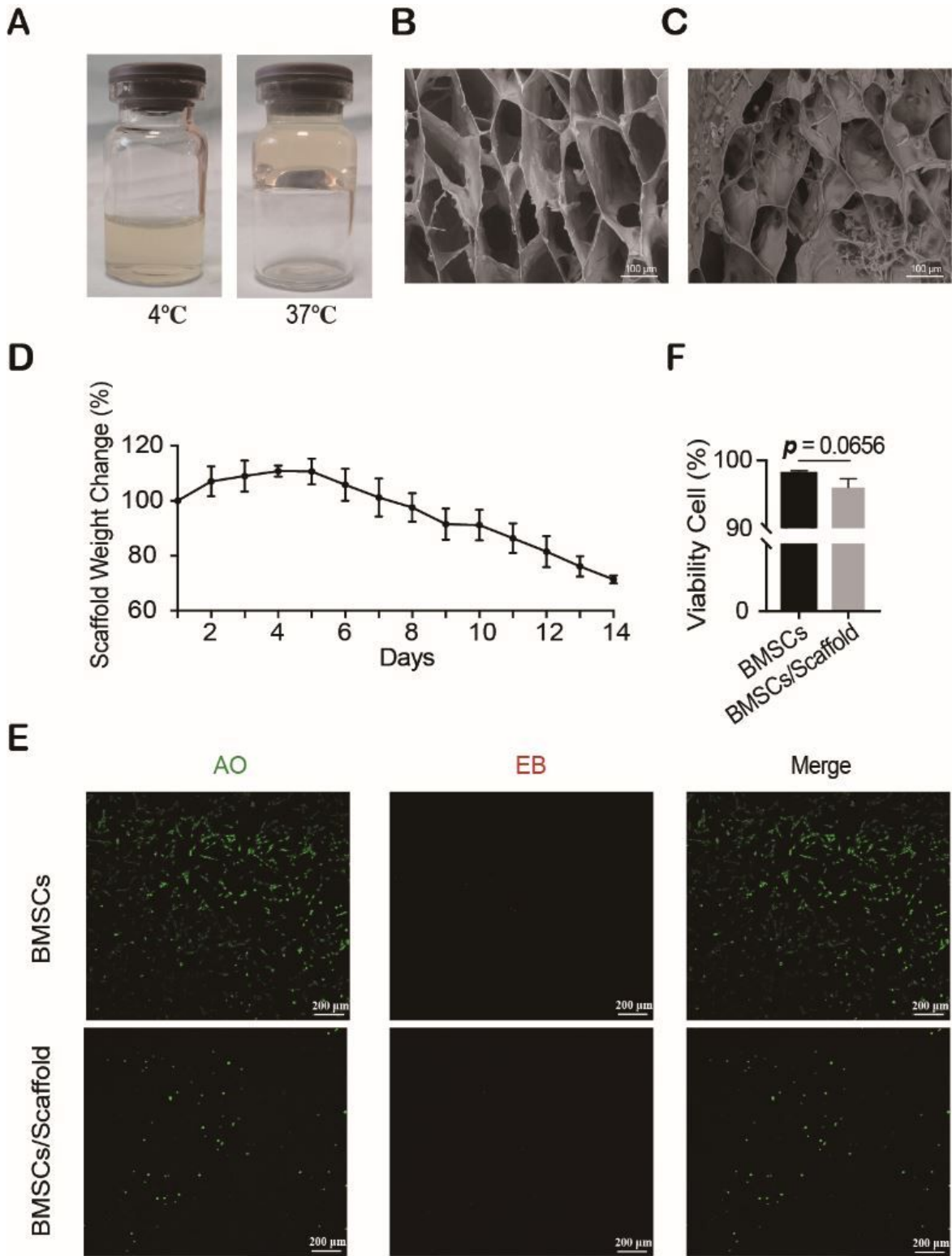


**Figure 2**

Pectin-Pluronic® F-127 scaffolds could provide 3D architecture for the attachment of BMSCs for the culture in vitro. (A) Image of Pectin-Pluronic® F-127 solution (Left) and scaffolds (Right). (B) The scanning electron microscope (SEM) images of the scaffold and BMSCs on the scaffolds (C). (D) In vitro cumulative degradation of Pectin-Pluronic® F-127 scaffolds. (E) Confocal images of the BMSCs by

AO/EB staining within scaffolds and without scaffolds for control. Green for live cells (AO) and red for dead cells (EB). (F) The apoptotic cell rate of BMSCs incubating within scaffolds and without scaffolds.

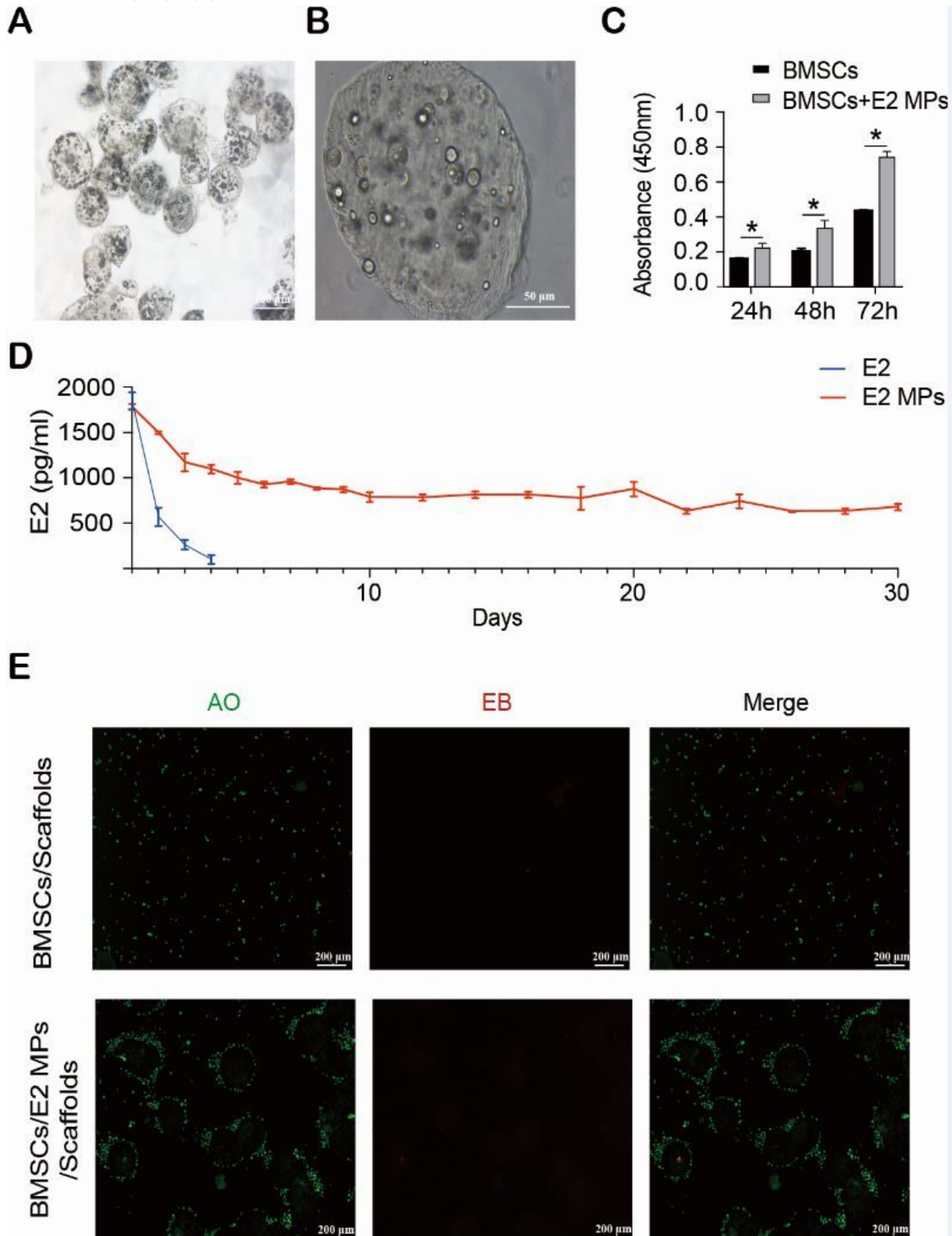


**Figure 3**

Pectin-based E2-loaded microcapsules (E2 MPs) serve as a reliable source of E2 to promote endometrial regeneration. (A) & (B) Images of E2 MPs in PBS. (C) BMSCs were cultured in the presence of E2 MPs, and cell vitality was measured by the cell counting kit-8 assay. (D) E2 MPs or E2 were incubated in

medium for 30 days. The medium was harvested to assay for the effective concentration of E2 using ELISA. (E) Confocal images of the BMSCs within scaffolds and BMSCs within E2 MPs/scaffolds. Staining of the cells: Green for live cells (AO) and red for dead cells (EB).

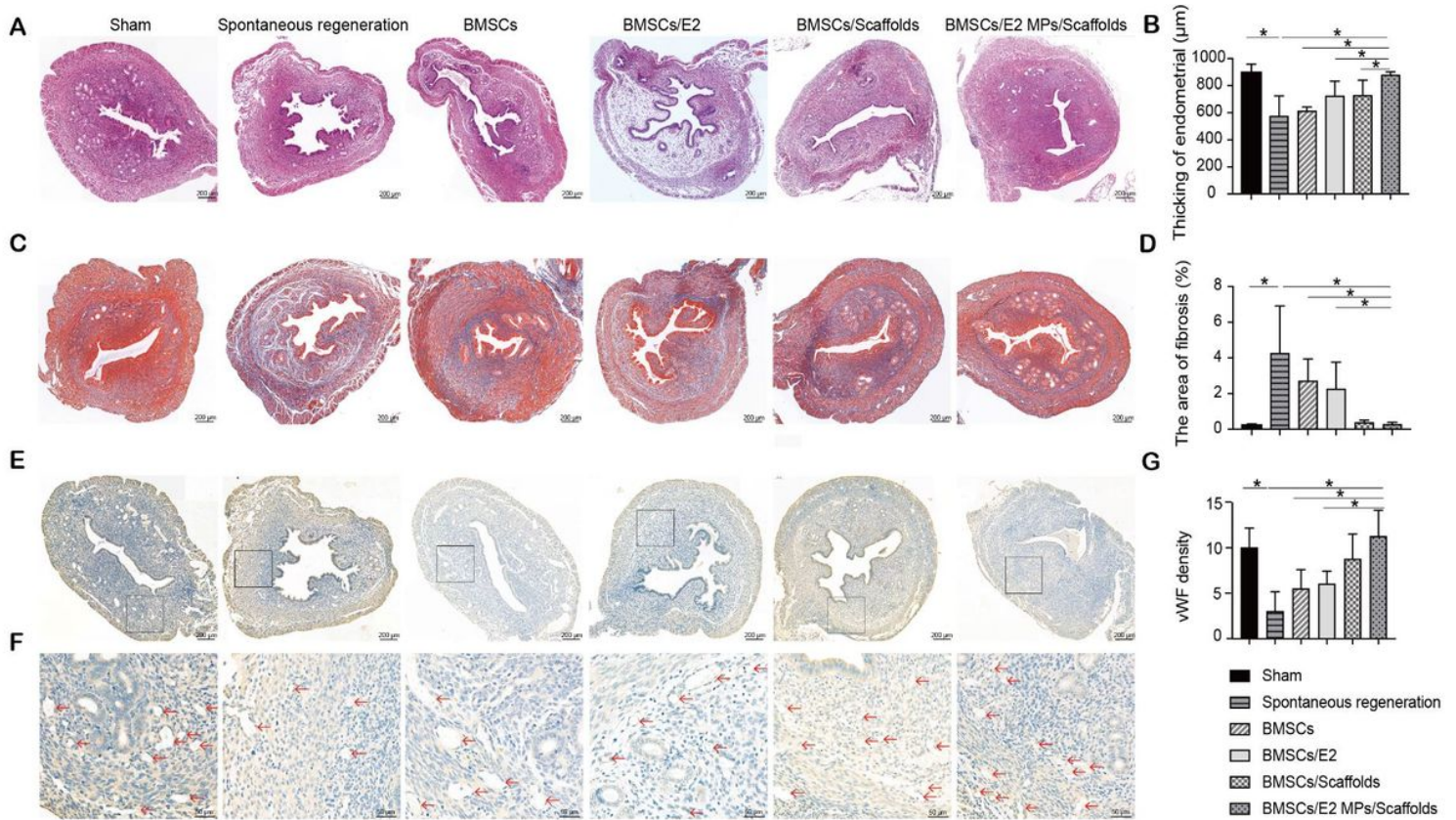


**Figure 4**

Transplantation of bone marrow mesenchymal stem cells and Pectin-based E2-loaded microcapsules on Pectin-Pluronic® F-127 scaffolds for mouse endometrial regeneration. (A) Histological structures and the thickness in the regenerative uterine horns after BMSCs/E2 MPs/scaffolds transplantation (HE staining). (B) Statistical analysis of the thickness of endometrial per section per mouse. (C) Masson's trichrome method stain of the collagen. (D) The percent of fibrosis areas in the endometrium per section per mouse. (E) Immunohistochemical staining of vWF expression for neovascularization in the regenerated endometria at four weeks after surgery. (F) Represented the part of regenerated endometrium of (E). Arrowheads indicate capillary vessels. (G) Number of capillary vessels per section. Data were presented as mean ± SEM. \* $p < 0.05$ .

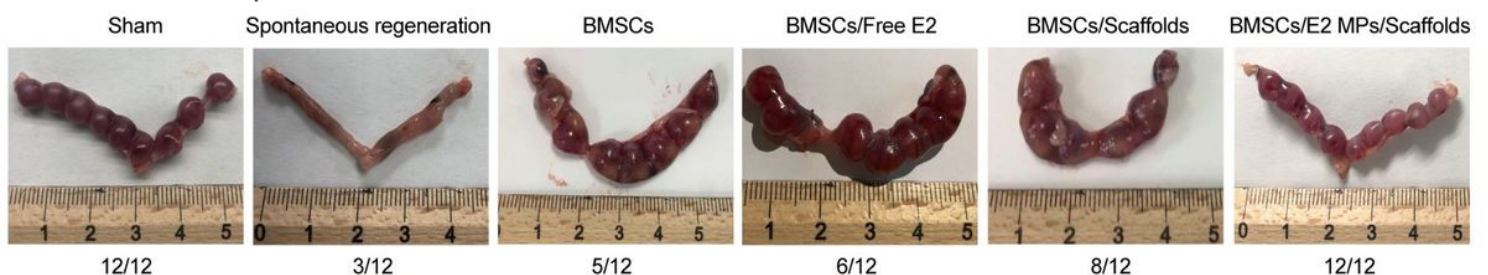


**Figure 5**

Embryo's implantation in different research groups after BMSCs/E2 MPs/scaffolds transplantation.

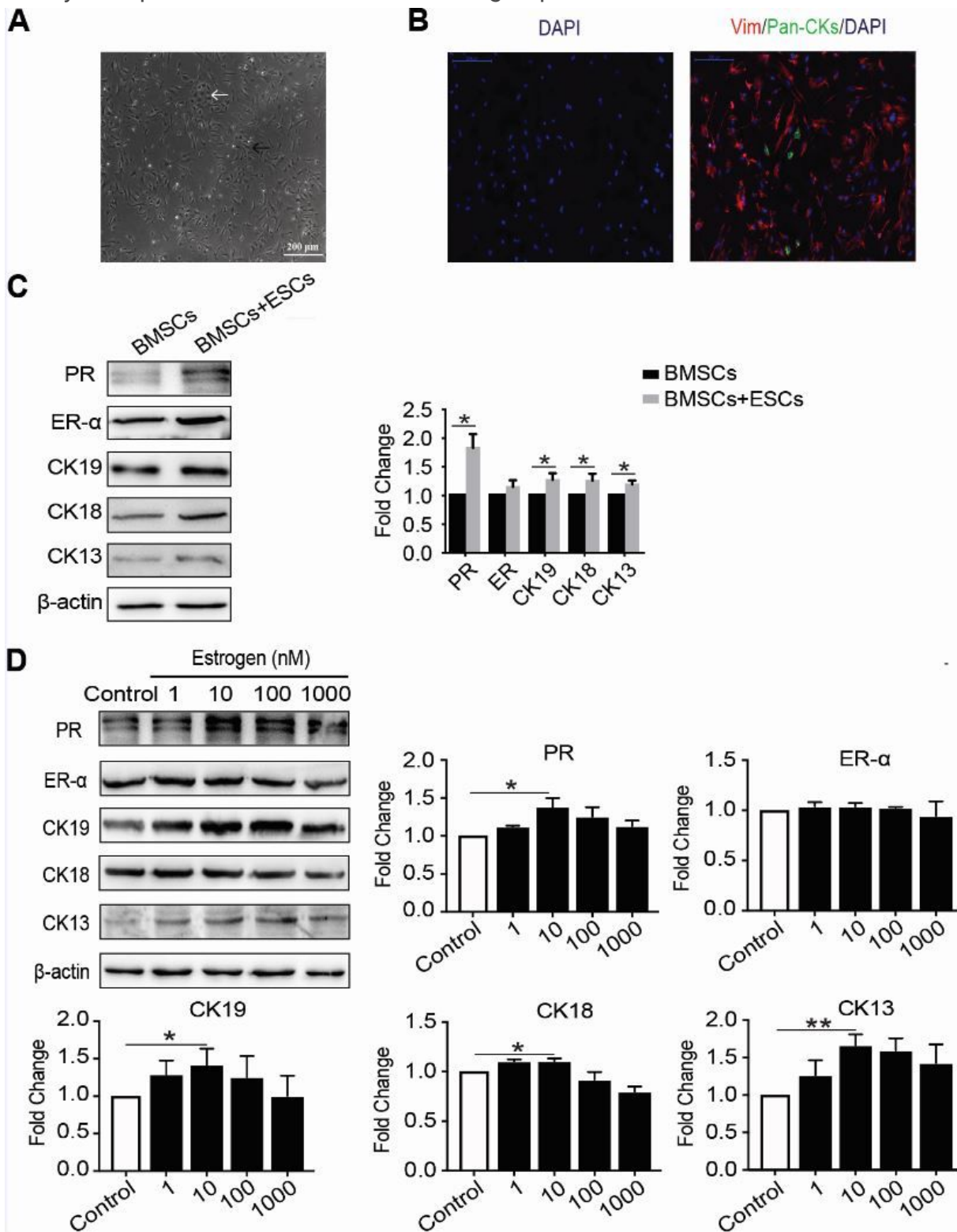


**Figure 6**

BMSCs differentiate into EEC-like cells in the coculture system. (A) Light microscope images of the ESCs (black arrow) and EECs (white arrow). (B) Vimentin/cytokeratin double staining on ESCs (Vim: red) and EECs (Pan-CKs: green) cultures. (C) Western blot analyses of PR, ER-α, CK19, CK18 and CK13 in cell lysates isolated from BMSCs co-cultured with or without ESCs. (D) BMSCs cocultured with ESCs with

different concentrations of E2 (0, 1, 10, 100, 1000 nM, respectively) in differentiation medium. Western blot analyses of PR, ER- $\alpha$ , CK19, CK18 and CK13 in cell lysates isolated from BMSCs to show the effect of concentration of E2 on the differentiation of BMSCs.  $\beta$ -actin was used as a loading control. Error bars represent SEM. \* $p < 0.05$ .

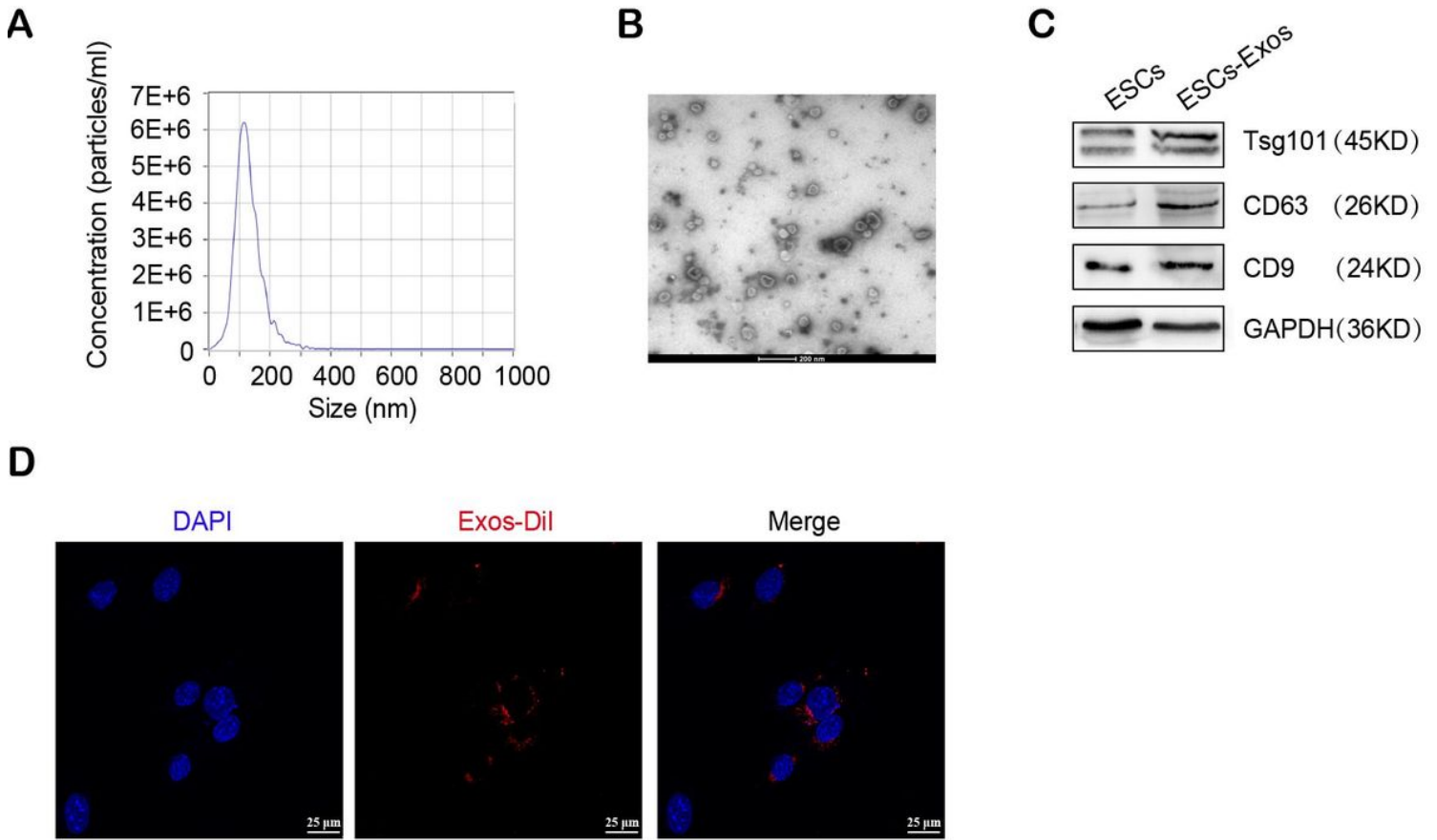


**Figure 7**

Characterization of Exosomes secreted by ESCs: (A) Particle size distribution measured by NTA. (B) Morphology observed by TEM. (C) Western blot of the exosome surface markers and cargo. (D) The BMSCs were collected for confocal microscopy to detect ESCs-Exos in BMSCs.

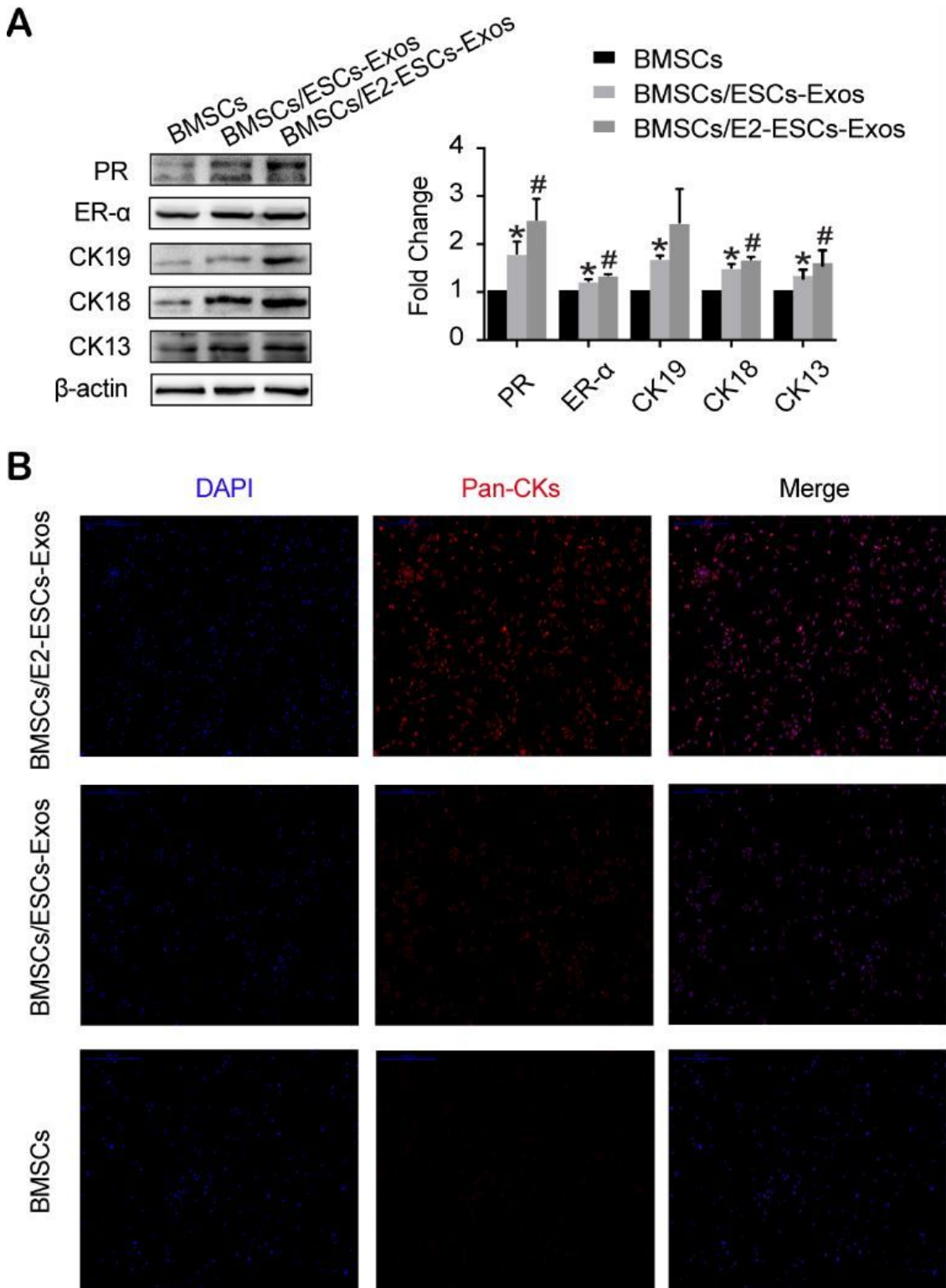


**Figure 8**

E2-Exos promoted BMSCs differentiation. (A) Western blot analyses of PR, ER- $\alpha$ , CK19, CK18 and CK13 in cell lysates isolated from BMSCs to show the effect of exosomes released from ESCs by E2 stimulation or not on the differentiation of BMSCs.  $\beta$ -actin was used as a loading control. Error bars represent SEM. \* $p < 0.05$  compared with BMSCs group. #  $p < 0.05$  comparing BMSCs/ESC-Exos and BMSCs/E2-ESC-Exos. (B) Immunofluorescent staining of BMSCs differentiation into EEC-like cells in the coculture system

with exosomes released from ESCs by E2 stimulation or not. Cells in the three groups stained with anti-Pan-CKs antibodies (red) and DAPI (blue). Scale bar: 500  $\mu\text{m}$ .

## Supplementary Files

This is a list of supplementary files associated with this preprint. Click to download.

- [supplementfigure.tif](#)